Materials Letters 355 (2024) 135545

Contents lists available at ScienceDirect

Materials Letters

journal homepage: www.elsevier.com/locate/matlet

Enhanced performance of electrospun poly(ethylene oxide)/reduced graphene oxide polymer electrolyte for lithium-ion batteries

J. Shahitha Parveen [a,*], M. Thirumurugan [b], M. Dhakshnamoorthy [c], S. Sathik Basha [d], R. Daulath Banu [a], V. Hari Shankar [a]

[a] Department of Polymer Engineering, B.S. Abdur Rahman Crescent Institute of Science and Technology, Chennai, India
[b] Department of Mechanical Engineering, B.S. Abdur Rahman Crescent Institute of Science and Technology, Chennai, India
[c] Faculty of Materials Science and Engineering, Jimma Institute of Technology, Jimma University, Jimma, Ethiopia
[d] Department of Physics, B.S. Abdur Rahman Crescent Institute of Science and Technology, Chennai, India

ARTICLE INFO

Keywords:
Reduced graphene oxide
Electrospinning
Gel polymer electrolytes
Impedance spectroscopy
Ionic conductivity
Lithium-ion battery

ABSTRACT

A novel polymer membrane based on electrospun poly(ethylene oxide) (PEO) incorporated with different concentrations of reduced graphene oxide (rGO) was prepared using the electrospinning technique. The electrospun PEO/rGO was incorporated with lithium ions to manufacture a gel polymer electrolyte (GPE) and sandwiched inside a coin cell. The electrochemical properties of PEO/rGO electrolytes confirmed good stability of the lithium cell, a satisfactory lithium transference number and improved ionic conductivity in the order of 10^{-3} S/cm. The GPE developed in this work is well suited for application in reliable, low-cost and eco-friendly energy storage technologies.

1. Introduction

The strong need for safer, lighter, low-cost and high-performance lithium-ion batteries has driven attention towards the development of GPE technology. Numerous researchers have developed polymer electrolytes from host polymers such as poly(vinylidene fluoride-co-hexafluoropropylene) (PVdF-HFP), poly(methyl methacrylate) (PMMA), poly(acrylonitrile) (PAN), poly(vinyl chloride) (PVC), polyethylene oxide (PEO) [1,2]. Among these, PEO receives much attention because of its ability to dissolve a variety of salts, electrochemical stability and beneficial structure for supporting ion migration [3]. It also possesses appealing properties such as the formation of more stable complexes with inorganic salts, good mechanical properties and stable chemical properties [4]. Neat PEO has conductivity in the order of 10^{-7} to 10^{-6} S/cm at room temperature [5] and is not suitable for practical applications. The order of conductivity of PEO is improved by the addition of rGO by suppressing its crystallization. A unique two-dimensional carbon material, rGO is used in energy storage systems such as lithium-ion batteries and supercapacitors. It is renowned for its high specific area, good chemical stability, exceptionally high electrical and thermal conductivity [5]. Electrospinning has been identified as a novel method for the development of highly porous membranes consisting of high surface to volume ratio nanofibers [6]. In this study, different concentrations of rGO incorporated in PEO solution were electrospun to form microfibrous membranes. The lithium hexafluorophosphate ($LiPF_6$) was incorporated into rGO/PEO microfibrous membranes to form gel polymer electrolytes and its excellent electrochemical performance in a coin cell makes the work novel.

2. Experimental details

2.1. Preparation of PEO/rGO based electrospun fibrous membranes

The rGO was prepared from graphite powder (Aldrich) using the modified Hummers method [7] (given in supplementary information S1). The PEO (average Mw ~ 4×10^5) (20 wt%) was dissolved in N, N-dimethylformamide and the mixture was stirred for 1 h at 50 °C. The prepared rGO of various compositions (0.1, 0.3, 0.5 and 0.7) parts per hundred (phr) were added to the mixture and then sonicated for 1 h. The sonication was carried out for the better dispersion of rGO onto the host polymer PEO. The solutions of PEO/rGO with various concentrations were further electrospun at 15 kV into fibrous membranes [8] (S2). The electrospun fibrous membranes were further investigated through fourier transform infrared spectroscopy (FTIR), thermogravimetric

* Corresponding author.
E-mail address: shahithaji@crescent.education (J. Shahitha Parveen).

https://doi.org/10.1016/j.matlet.2023.135545
Received 9 August 2023; Received in revised form 22 October 2023; Accepted 7 November 2023
Available online 8 November 2023

analysis (TGA), differential scanning calorimetry (DSC) and scanning electron microscopy (SEM) (S3).

2.2. Fabrication of coin cell

The PEO/rGO-based polymer electrolytes were prepared by soaking the fibrous membranes in an electrolyte solution of 1 M $LiPF_6$ in ethylene carbonate/ dimethyl carbonate/ diethyl carbonate solution for 1 h. The composite cathode was prepared by dissolving 5 wt% poly (vinylidene fluoride) in N-methyl-2-pyrrolidone. The mixture was added to 10 wt% conductive carbon and 85 wt% lithium iron phosphate ($LiFePO_4$) to form viscous slurry. The slurry was then coated with aluminum foil and placed in a vacuum oven at 120 °C for 12 h [9]. The PEO/rGO gel polymer electrolytes were sandwiched between the lithium (ribbon) anode and lithium iron phosphate composite cathode in a coin cell standard CR2032 (MTI Corporation, United States) in a glove box filled with argon gas (H_2O < 1 ppm).

3. Results and discussion

FT-IR spectroscopic analysis was done for PEO and PEO/rGO and the spectra are presented in Fig. 1(a). The spectra for neat PEO show C-H stretching mode at 2879 cm^{-1}, CH_2 scissoring mode at 1466 cm^{-1}, symmetric CH_2 wagging mode at 1352 cm^{-1}, CH_2 twisting mode at 1276 cm^{-1}, CH_2 rocking at 830 cm^{-1} and C-O-C bending at 524 cm^{-1} [10]. The occurrence of a triple peak of C-O-C stretching with maximum intensity at 1097 cm^{-1} confirms the presence of the semi-crystalline phase of PEO. The existence of a band at 944 cm^{-1} is the distinctive peak in supporting the gauche conformations of $–CH_2$ $–CH_2$ groups for the helical conformation of neat PEO [11]. There is no noticeable difference in the FTIR spectra of PEO and PEO/rGO since PEO is blended with rGO.

The Fig. 1 (b) reveals an endothermic peak at 66.2 °C, corresponding to the melting of the crystalline phase of PEO. Upon incorporation of rGO, the melting temperature (T_m) of the PEO/rGO fibrous membranes is shifted to a slightly lower temperature range of 64 °C. The crystallinity of PEO was found to decrease by the addition of rGO to PEO. The melting enthalpy (ΔH_m) of both PEO and PEO/rGO are 177.9 J/g and 115.34 J/g. The ΔH_m decreases with the addition of rGO and generates more amorphous domains improving the migration of ions.

The Fig. 1(c) shows the thermal stability of fibrous membranes.The reduction process of hydrazine removes oxygen-containing functional groups and it is evident from the increased thermal stability of PEO/rGO membranes. It was observed that the initial decomposition temperature of PEO was 354 °C, while the onset decomposition temperature of PEO (0.1 phr, 0.3 phr,0.5 phr,0.7 phr rGO) was 369 °C, 374 °C, 384 °C and 420 °C respectively. The PEO polymer matrix and rGO interact strongly to improve thermal stability.

The morphology of the fibrous membranes was analyzed using SEM. The electrospun PEO and PEO/rGO fibrous membranes in the Fig. 2(a), (b) and (c) have a rich microporous structure and exhibit interconnected multi-fibrous layers. The PEO/rGO fibrous membranes with mean pore

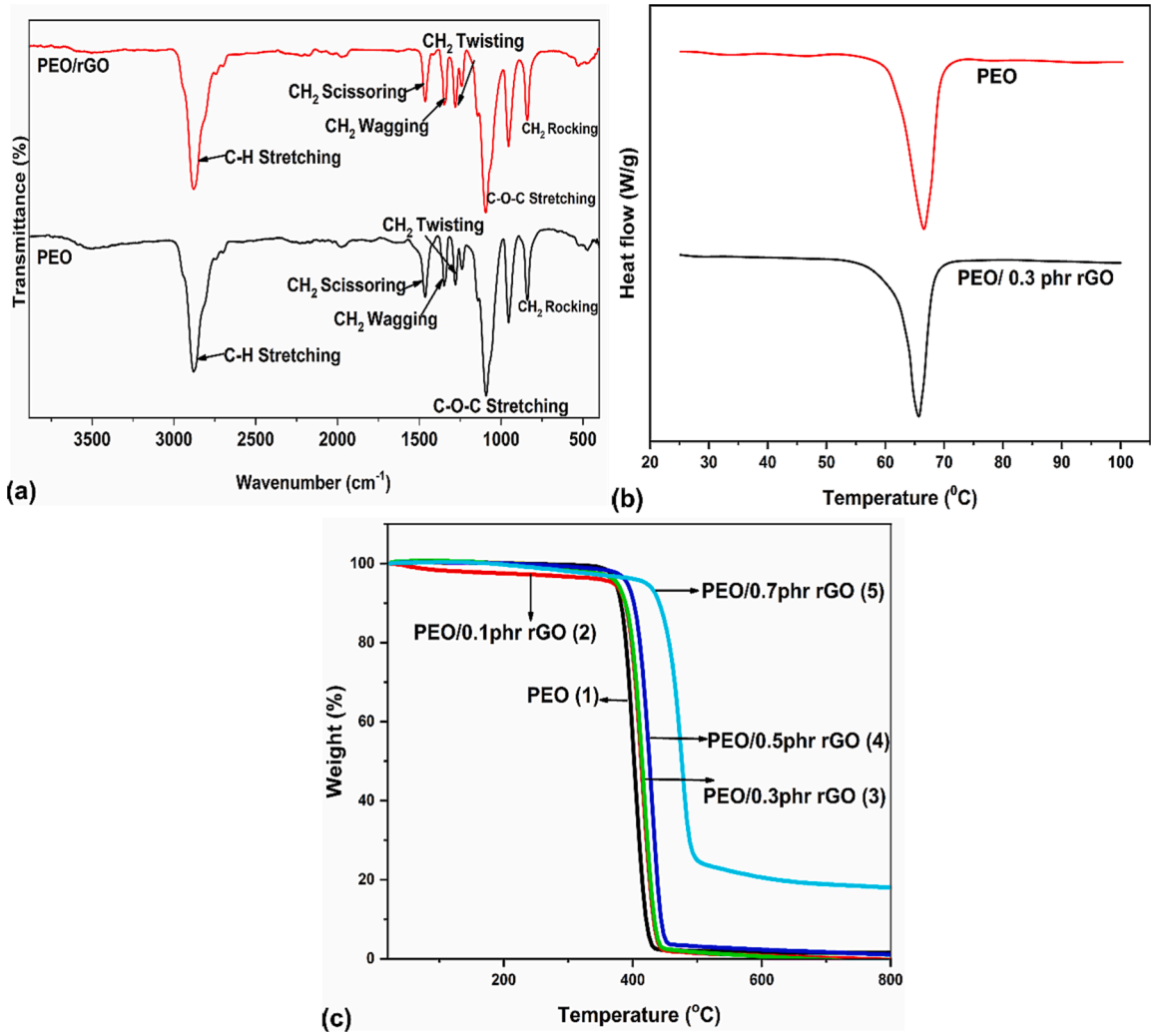

Fig. 1. (a) FTIR spectra, (b) DSC thermogram, (c) TGA thermogram.

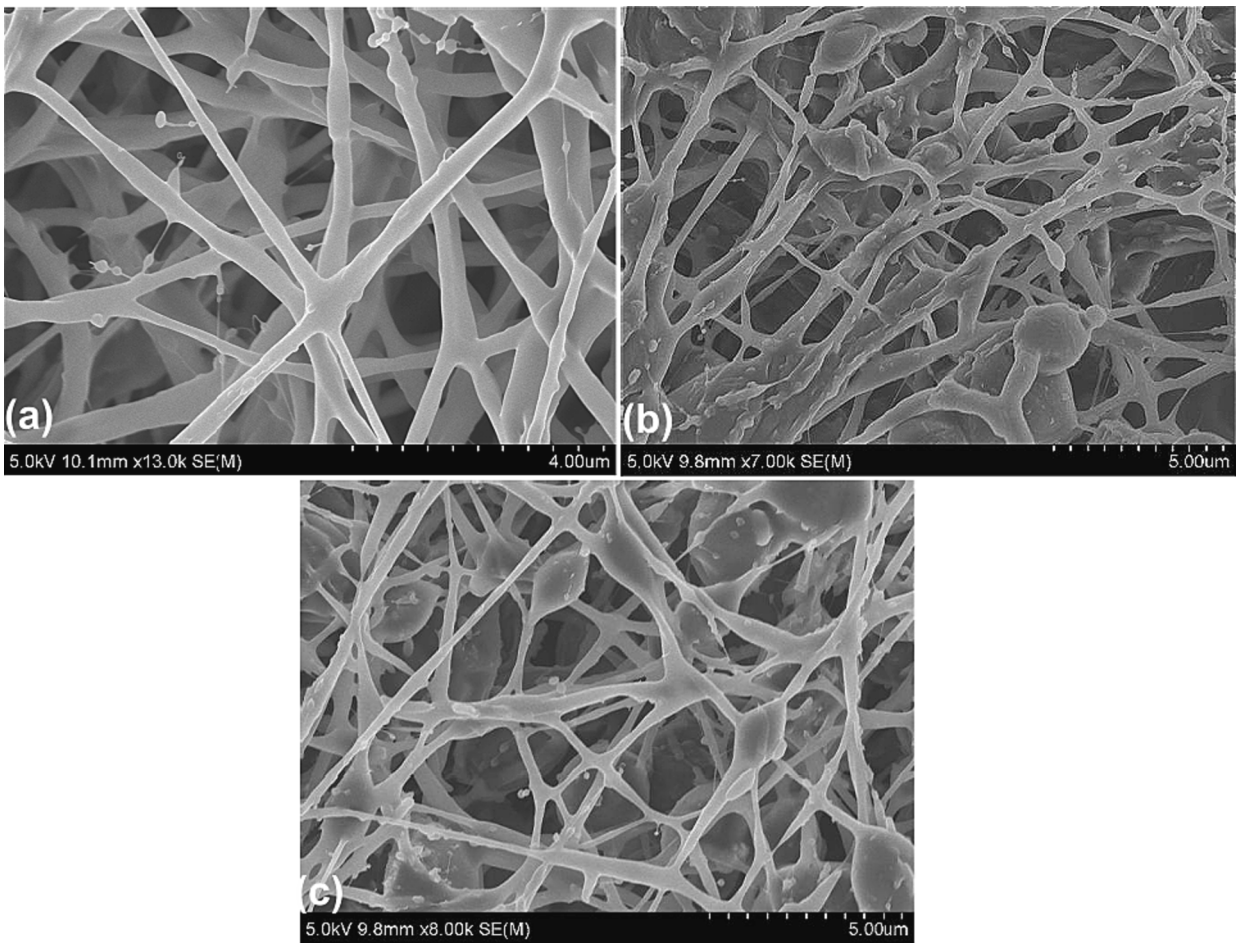

Fig. 2. SEM micrograph of electrospun (a) neat PEO (b) PEO/0.3 phr rGO (c) PEO/0.7 phr rGO.

sizes (MPS) were found to range from 1.2 to 1.8 μm. Beads have been identified on these surfaces of the fibrous membranes, confirming the existence of rGO and the size of the beads were measured as ~ 0.77–0.92 μm.

All concentrations showed the same pattern, and rGO was found to be disseminated among the polymer fibers. The diameter of the fibrous membranes ranges from 120 to 250 nm, and the inclusion of the rGO caused a highly noticeable bulging of the fibrous membrane (S4).The formation of the beads causes low interfacial interaction between rGO and the polymer matrix which encourages rGO to cluster rather than conform to the shape of the matrix. By loading extremely low quantities of rGO, the formation of beads was controlled. Thus the SEM images depict the proper orientation of microfibrous membranes.

From the Table 1, it was inferred that with the increase in the rGO content, the PEO/rGO fibrous membrane has increased porosity leading to greater electrolyte solution absorption and influences ionic mobility. By applying DC polarization and the Bruce-Vincent equation, the transference number of the PEO/rGO gel polymer electrolytes is calculated and tabulated [3]. The increase in the transference number indicates the increase in charge carriers of the PEO/rGO fibrous membranes. The ionic conductivity of PEO/rGO fibrous membranes was measured using impedance spectroscopy in the frequency ranges of 1 Hz to 100 kHz. Ionic conductivity for PEO/0.1 phr rGO is on the order of 10^{-6} Scm^{-1}, however, the addition of rGO content improved the ionic conductivity to the order of 10^{-3} S cm^{-1}. The mobility of the conducting ions is effectively facilitated by the interaction between the rGO and PEO chains leading to an increase in ionic conductivity.

The temperature dependence of ionic conductivity of PEO/rGO shown in Fig. 3(a) obeys Arrhenius law. The activation energy (E_a) obtained from the Arrhenius equation is shown in Table 1.The reduction in E_a with an increase in rGO content enhances the ionic conductivity and rGO functions as mobile charge carriers in PEO/rGO electrolytes.

Using linear sweep voltammetry, the electrochemical stability window of PEO/rGO polyelectrolytes was determined. Fig. 3b demonstrates the electrochemical stability of the Li/GPE/$LiFePO_4$ cell with gel polymer electrolyte (GPE) based on PEO/0.3 phr rGO polyelectrolytes up to 4.8 V and and the cell with PEO/0.7 phr rGO was stable up to 5.3 V. The incorporation of rGO content in PEO increases the amorphous phase thereby increasing the porosity, electrolyte absorption, and ionic conductivity and making the coin cell battery electrochemically stable.

Table 1
Properties of fibrous membranes.

PEO/rGO fibrous membranes	Porosity (%)	Electrolyte uptake (%)	Transference number	Ionic Conductivity (Scm^{-1})	Activation Energy (kJ/mol)
PEO/0.1 phr rGO	70	360	0.74	3.72×10^{-6}	25.2
PEO/0.3 phr rGO	72	372	0.79	3.46×10^{-5}	23.6
PEO/0.5 phr rGO	74	380	0.80	2.71×10^{-4}	21.8
PEO/0.7 phr rGO	78	392	0.82	2.42×10^{-4}	21.4

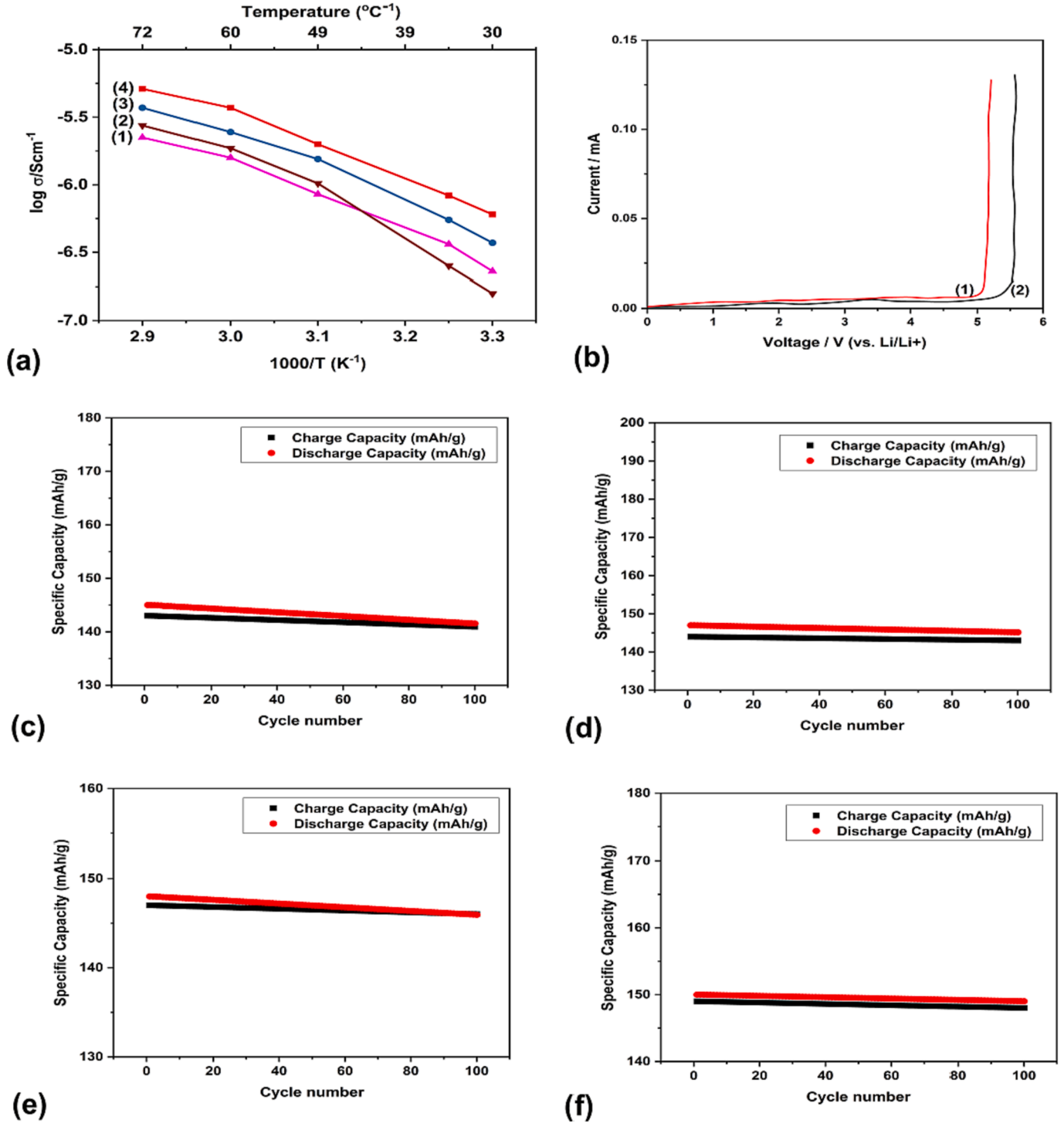

Fig. 3. (a) Arrhenius plots of PEO blended with (1) 0.1 phr rGO, (2) 0.3 phr rGO, (3) 0.5 phr rGO, (4) 0.7 phr rGO (b) Electrochemical window of Li/GPE/$LiFePO_4$ cells with GPE based on electrospun PEO with (1) 0.3 phr rGO, (2) 0.7 phr rGO, Cycling performances of Li/GPE/$LiFePO_4$ cells with GPE based on PEO (c) 0.1 phr rGO, (d) 0.3 phr rGO, (e) 0.5 phr rGO, (f) 0.7 phr rGO fibrous membranes.

Under constant voltage conditions, the prototype cell with the PEO/rGO GPE displayed excellent steady charge–discharge behavior and minimal capacity loss. The charge–discharge curves of the cells with PEO/rGO electrolytes are shown in Fig. 3(c-f). The cell with PEO/rGO (0.1phr, 0.3phr, 0.5pr and 0.7phr) has an excellent discharge capacity of 145 mAh g^{-1}, 147 mAh g^{-1}, 148 mAh g^{-1} and 150 mAh g^{-1} respectively and delivers excellent performance.

4. Conclusion

In this work, PEO/rGO GPE fibrous membranes were prepared successfully using electrospinning techniques and the addition of rGO to the PEO matrix increases the ionic conductivity and provides a good affinity between the electrode and the polymer electrolyte. Due to the amount of electrolyte solution absorbed within the polymer matrix, the cells are observed to have greater retention capacity and interfacial properties than neat PEO. Higher porosity and enhanced electrolyte uptake

improve the discharge capacity of the cells. Thus, the PEO/rGO based GPE is a promising candidate for high-performance lithium-ion batteries.

CRediT authorship contribution statement

J. Shahitha Parveen: Conceptualization, Methodology, Validation, Formal analysis, Investigation, Writing – original draft. **M. Thirumurugan:** Validation, Visualization, Writing – review & editing. **M. Dhakshnamoorthy:** Validation, Writing – review & editing. **S. Sathik Basha:** Resources, Writing – review & editing. **R. Daulath Banu:** Resources, Writing – review & editing. **V. Hari Shankar:** Conceptualization, Resources, Investigation, Project administration, Supervision, Writing – review & editing.

Declaration of Competing Interest

The authors declare that they have no known competing financial interests or personal relationships that could have appeared to influence the work reported in this paper.

Data availability

Data will be made available on request.

Acknowledgment

We thank the Department of Science and Technology, Ministry of Science and Technology, India for funding our research work.

Appendix A. Supplementary data

Supplementary data to this article can be found online at https://doi.org/10.1016/j.matlet.2023.135545.

References

[1] Adhigan Murali, Mohan Sakar, Sahariya Priya, V. Vijayavarman, Sadanand Pandey, Ryansu Sai, Yu Katayama, M. Abdul Kader, Kothandaraman Ramanujam, Mater. Lett. 313 (2022) 131764, https://doi.org/10.1016/j.matlet.2022.131764.
[2] C.-C. Yang, S.-J. Lin, Mater. Lett. 57 (2002) 873–881, https://doi.org/10.1016/j.matlet.2022.131764.
[3] S. Zhao, Q. Wu, W. Ma, L. Yang, Front. Chem. 8 (2020) 640, https://doi.org/10.3389/fchem.2020.00640.
[4] A. Karmakar, A. Ghosh, Curr. Appl. Phys. 12 (2012) 539–543, https://doi.org/10.1016/j.cap.2011.08.017.
[5] Z. Zhong, Q. Cao, B. Jing, X. Wang, X. Li, H. Deng, Mater. Sci. Eng. B 177 (2012) 86–91, https://doi.org/10.1016/j.mseb.2011.09.008.
[6] A.G. Olabi, M.A. Abdelkareem, T. Wilberforce, E.T. Sayed, Renew. Sustain. Energy Rev. 135 (2021), 110026, https://doi.org/10.1016/j.rser.2020.110026.
[7] T. Panneerselvam, A. Rajamani, N. Janani, R. Murugan, S. Sivaprakasam, Ionics 29 (2023) 1395–1406, https://doi.org/10.1007/s11581-023-04905-3.
[8] S. Park, R.S. Ruoff, Nat. Nanotechnol. 4 (2009) 217–224, https://doi.org/10.1038/nnano.2009.58.
[9] A.K. Solarajan, V. Murugadoss, S. Angaiah, J. Appl. Polym. Sci. 134 (2017) 45177, https://doi.org/10.1002/app.45177.
[10] P.A.R. Jayathilaka, M.A.K. Dissanayake, I. Albinsson, B.-E. Mellander, Electrochim. Acta 47 (2002) 3257–3268, https://doi.org/10.1016/S0013-4686(02)00243-8.
[11] Z. Shen, G.P. Simon, Y.-B. Cheng, Polymer. 43 (2002) 4251–4260, https://doi.org/10.1016/S0032-3861(02)00230-6.